Thermal Performance of Micro-Pulsating Heat Pipe

A Bakhirathan, R Giridhar, K D P Pavan Kumar, Gangadhara Kiran Kumar Lachireddi

Abstract: ***In this study, thermal performance of MPHP is investigated computationally. A case with 0.7mm hydraulic diameter with 7 turns is considered for the study. Simulation is carried out using ANSYS-FLUENT® software by considering water as working fluid with the help of VOF model. Computational study shows the oscillation of fluid inside and formation of new vapor slugs. The heat input is varied from 1.2 W to 4.8 W in the step of 1.2. Flow circulation inside the MPHP is not unidirectional and frequently changes with the pressure disturbance created in the channels. The temperature profile from computational study shows the startup condition is changing with heat input. Thermal resistance of the MPHP decreases with increase in heat input and the corresponding thermal resistance found to be varied from 3.94 to 3.65 K/W.***

Index Terms**: *Fill ratio, Micro-Pulsating Heat Pipe, Thermal Management, Thermal Resistance.***

NOMENCLATURE

ρ = Density
μ = Viscosity
k = Thermal conductivity
C_p = Specific heat
σ = Surface tension
α = Volume fractions
Q = Heat input (W)
R = Thermal resistance (K/W)
Subscripts
l = of liquid phase
v = of vapor phase

I. INTRODUCTION

In recent days, thermal management of electronics becoming a significant area of research because of the technological advancement happening in electronics industry. All the electronics industry especially semiconductor and microprocessor industry follow the Moore's law, states that decreasing the size of the processor increases the performance i.e., faster response. This technological advancement results in increase of transistor density, tuning the clock signals, miniaturization of the devices which leads to dissipation of high heat flux at chip level. Local hot spots created by the transistor is the key reason for high heat flux which ultimately increases the junction temperature of the microprocessor and affects the reliability of the device. In this case, maintaining the junction temperature within the limit even at the higher heat flux is a challenge for thermal engineers. The non-uniformity in an operating temperature of the chip leads to a decrease in performance of the electronic component. There is a 10% decrease in performance in the electronic components for every 2 °C rise in operating temperature [1]. Already several methods of cooling such as air or water cooling, spray cooling, heat pipe and jet impingement have been employed to achieve uniform temperature condition. Now-a-days along with high heat flux, space constraints are another problem faced by electronic industry to employ the cooling system, which results in higher complexity in manufacturing the system and affects the performance as well. According to the iNEMI roadmap it is estimated that chip could generate heat flux around 400W/cm^2 by 2020.

The heat pipe is a passive heat transfer device, which is employed to cool the electronic devices to transfer the generated heat. In conventional heat pipe wick structure is used to return the condensate to evaporator. The thermal management is becoming a challenge for the compact sizes of electronics components such as processor by using the conventional heat pipe. Much research would have been carried out to meet a need of effective thermal management system. Adding to this pulsating heat pipe (PHP) was first patented [2] with capillary tubes in the form of serpentine arrangement, in which the liquid slugs and vapor plugs are present in the form of train. The wick structure is absent in this heat pipe, which makes it different from conventional heat pipe, so flow inside the heat pipe is driven majorly by surface tension force and there is no counter flow, which predominantly reduce the vapor and liquid shear. When the heat is supplied at the evaporator, bubbles start to expand and in the condenser section bubble releases latent heat and collapse. Due to this expansion and contraction of the bubble, oscillating motion is attained in the PHP. The performance of PHP depends on several factors such as fill ratios (FR), diameter/channel dimensions, no. of turns of the capillary tube and length of evaporator and condenser section. Till date, there is no clear information in designing the PHP other than critical diameter constraints given by Bond Number (Bo) range which is function of buoyance force and surface tension force, where 1≤ Bo≤ 2

Revised Manuscript Received on October 20, 2019.
***** Correspondence Author
Gangadhara Kiran Kumar Lachireddi*, Mechanical Engineering Department, National Institute of Technology - Calicut, Kozhikode, Kerala, India.

indicates the surface tension dominant condition which results in increasing capillary action of the tube. Most of the investigation on PHP are carried with in this range and concluded that suits for electronic cooling but when considering the space occupied by this PHP system, it is more than the existing heat sink setup, example heat sink employed in on-chip cooling. Bo ≤ 1, condition, makes the heat pipe to fall into category of Micro Heat Pipe (MHP) [3], [4].

Computationally investigation of conventional pulsating heat pipe as a preliminary study to understand the thermo-hydrodynamic operations. Zhao et al. [5] studied the influence of initial vacuum pressure condition for different pressure values of PHP and found that variation of oscillating pressure difference is very less. Zhang et al. [6] Studied the chaotic behavior of PHP with two turns and depicted the temperature profile at evaporator and discussed about bubble generation. Zhang et al. [7] studied the behavior of PHP computationally with constant temperature boundary condition in both evaporator and condenser.

In this study Bo≤1 can be used as a condition to determine the critical diameter of PHP thereby it reduces the hydraulic diameter, which in turn PHP will fall in the category of Micro Pulsating Heat Pipe (MPHP) and oscillation behavior of micro channel pulsating heat pipe is investigated for 0.7mm hydraulic diameter with 7 turns at various heat input. Finite volume-based software ANSYS FLUENT® - 19.1 is used to carry out the numerical investigation on MPHP.

II. MODELLING AND SIMULATION OF MPHP

Two-dimensional structure of MPHP is considered for investigating the parameter. Figure 1 shows the computational domain and the dimensions of the MPHP. The dimension limits of MPHP with respect to its length and height is fixed by considering on-chip cooling system, 2U narrow high performance heat pipe-heat sink which is presently employed in Intel [8]. Therefore, maximum allowable length and height of the system is 110 mm and 64mm. Based on this, MPHP with 0.7 mm capillary dimension are considered to investigate the performance. The maximum number of turns is limited by the length constraints along with minimum radius which should be maintained while bending the capillary tube without rupturing the channel which results in 7 turns for 0.7 mm.

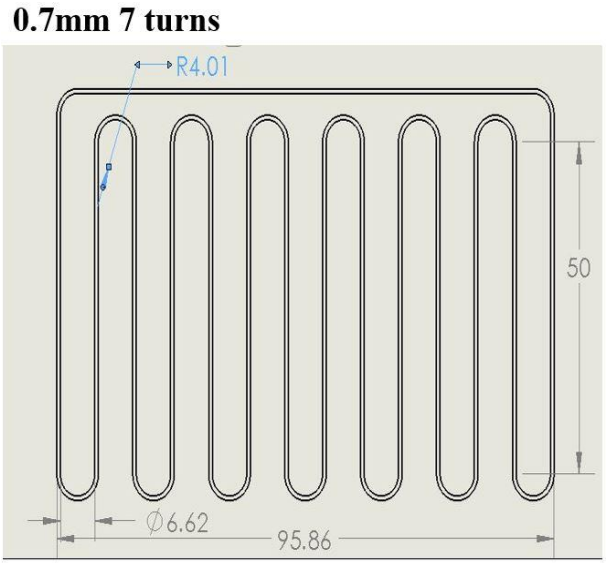

Figure 1: Computational domain of 0.7 mm channel

MPHP consist of evaporator and condenser section. The entire bottom U-portions are considered as evaporator and subjected to constant heat flux boundary condition. Remaining portion of MPHP other than evaporator is considered as condenser section, boundary condition is different for middle portion and top portion of MPHP. All the top U-portion is subjected to constant wall temperature condition of 300K. In between top and bottom U-portion, middle portion is subjected to free convection of 10 W/m^{2}K. Discretization is based on finite volume approach and transient pressure based solver is used. Gradients are calculated by least square cell method, SIMPLE algorithm is used to solve pressure velocity coupling. Two eulerian phase is used in volume of fluid(VOF) model with implicit scheme. PRESTO! and compressive is used to solve the pressure and volume fraction equation. Water is considered as a working fluid. Volume of Fluid (VOF) is a surface tracking technique which is used to simulate two phase flow for a fixed Eulerian mesh. It is suitable for two or more immiscible fluids by which the position of the interface between the fluids can be studied. It is formulated based on the condition that phases which exist in the system should not interpenetrate. Each and every phase in the system will have an individual volume fraction α. As the ANSYS-FLUENT® works on the basis of control volume technique, each cell in the computational domain is considered as control volume. Summation of all the liquid fraction of the individual cell is equal to one. All the properties and variables of the fields are calculated based on the volume-averaged condition, provided volume of fraction of each phase is known at every point. Depending on the volume fraction existing in the cell, the variables and properties of each phase is representing either single phase is filled in the control volume or multiphase co-exist in the control volume. The volume fraction of q in the cell is represented as α_q. Volume fraction of qth fluid will have local value (α_q), based on this variables and properties will be assigned to each control volume i.e., each cell in the domain. By solving the continuity equation, the interfaces between the phases are tracked

for the one or more phases. Considering q[th] fluid phase, the continuity equation will be in the form represented below.

$$\frac{1}{\rho_q}\left[\frac{\partial}{\partial t}(\alpha_q\rho_q) + \nabla.(\alpha_q\rho_q\vec{v_q}) = S_{\alpha_q} + \sum_{p=1}^{n}(m_{pq} \dot{-} \dot{m_{qp}})\right] \quad (1)$$

Where $\dot{m}$ represent the mass transfer, suffix pq and qp in the above equation indicates the reaction between the two phases. S_{α_q} is the source term in the equation, its valued to be zero. The volume fraction equation will not be solved for the primary phase i.e.; the primary phase volume fraction will be computed based on the following constraint

$$\sum_{q=1}^{n}\alpha_q = 1 \quad (2)$$

Both explicit and implicit time discretization method can be used to solve volume fraction equation. Implicit scheme is used to solve the volume fraction. To attain the values of face fluxes for all individual cells including the cells near interface in computational domain, first order and second order upwind, Compressive, Modified HRIC schemes are used.

$$\frac{\alpha_q^{n+1}\rho_q^{n+1} - \alpha_q^n\rho_q^n}{\Delta t}V + \sum_f\left(\rho_q^{n+1}U_f^{n+1}\alpha_{q,f}^{n+1}\right) = \left[S_{\alpha_q} + \sum_{p=1}^{n}(m_{pq} \dot{-} \dot{m_{qp}})\right]V \quad (3)$$

The above equation requires the α_q values at the current time step, a standard scalar transport equation is solved iteratively at each time step for the secondary-phase volume fractions.

where the time step is represent with n+1 index and for previous time step n is the index, face value of the q_{th} volume fraction is denoted as $\alpha_{q,f}$, V is the volume of cell, and U_f is the volume flux through the face based on normal velocity.

The phases present in each cell determines the properties present in the transport equation. The density and viscosity in each cell are given by

$$\rho = \alpha_v\rho_v + (1-\alpha_v)\rho_l \quad (4)$$

$$\mu = \alpha_v\mu_v + (1-\alpha_v)\mu_l \quad (5)$$

The velocity field attained by solving the momentum equation throughout the domain is shared among the interacting phases. Because of this, the velocity calculated near the interface is not accurate and leads to large velocity difference between the interacting phases.

$$\frac{\partial}{\partial t}(\rho\vec{v}) + \nabla.(\rho vv) = -\nabla p + \nabla.[\mu(\nabla v + \nabla v^T)] + \rho g + F \quad (6)$$

The momentum equation, shown above is dependent on the volume fractions of all phases through the properties ρ and μ.

$$\frac{\partial}{\partial t}(\rho E) + \nabla.\left(\vec{v}(\rho E + p)\right) = \nabla.\left(k_{eff}\nabla T\right) + S_h \quad (7)$$

In VOF, energy and temperature are considered as mass-averaged variable in the domain.

$$E = \frac{\sum_{Q=1}^{n}\alpha_q\rho_q E_q}{\sum_{q=1}^{n}\alpha_q\rho_q} \quad (8)$$

where E_q for each phase depends on the specific heat of that phase and the temperature. The properties ρ and k_{eff} (effective thermal conductivity) of the existing phases. Using the local gradients in surface normal at the interface, the surface curvature is computed. Let **n** be the surface normal, defined as the gradient of α_q, the volume fraction of the q[th] phase.

$$\boldsymbol{n} = \nabla\alpha_q \quad (9)$$

$$\boldsymbol{k} = \nabla.\hat{\boldsymbol{n}}$$

Where, k is the curvature. As the surface tension is function of pressure jump and this force at particular surface can be written using the divergence theorem. Surface tension force is expressed in the form of volume force and added as source term in the momentum equation. The volumetric force represented below.

$$F_{vol} = \sum_{pairs\,ij,i<j}\sigma_{ij}\frac{\alpha_i\rho_i k_j\nabla\alpha_j + \alpha_j\rho_j k_i\nabla\alpha_i}{\frac{1}{2}(\rho_i + \rho_j)} \quad (10)$$

$k_i = -k_j$ and $\nabla\alpha_i = -\nabla\alpha_j$ are the representation of vapor-liquid phase existing in the cell. Volume average density can be calculated using below equation.

$$F_{vol} = \sigma_{12}\frac{\rho k_1\nabla\alpha_2}{\frac{1}{2}(\rho_1 + \rho_2)} \quad (11)$$

Surface tension dominated study has a significant effect on the element type. According to Zhang et al. [6], hexahedral and quadrilateral mesh is preferred in case of two dimensional and three-dimensional domains for surface tension dominated problem. Therefore, proper mesh with all quadrilateral elements should be chosen for simulation shown in figure 2.

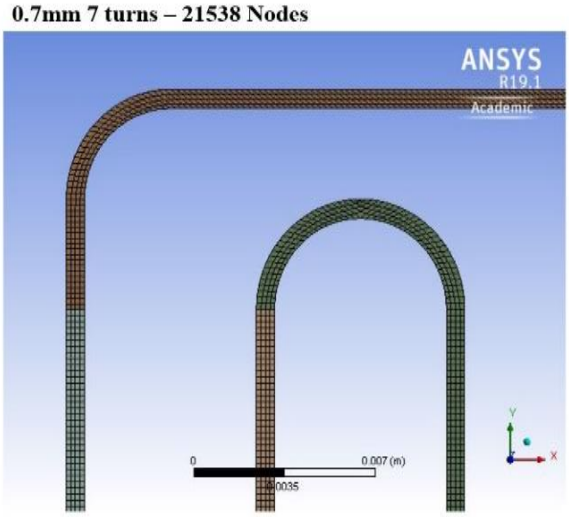

Figure 2: Quadrilateral mesh

Based on this condition, the final mesh size is fixed to simulate the MPHP. In MPHP average skewness factor for the mesh is maintained at 0.1 to avoid divergence of solution. Input heat flux is the only boundary condition changes for every case. The heat input ranges from 1.2 W to 4.8 W. Implicit scheme with time step of 0.005 is used to simulate the MPHP.

III. RESULTS AND DISCUSSION

The liquid fraction contours at critical situations based on flow parameters for the MPHP is

shown in Figure 3 to 11. The simulation is carried out for 60 s, because of the time complexity in solving the problem. Liquid fraction contour helps to understand how the oscillation starts inside the MPHP and the vapor bubble formation, its expansion and collapsing nature on releasing the heat. In this study water is the working fluid and initial contour at t = 0s, initial condition of MPHP shows the water in the bottom U-portion (red in contour) and water-vapor (blue in color) in the top position. At t = 0s, red-blue junction in the liquid fraction contour shows the separation of liquid and vapor phase. At t = 1s the boiling of liquid start to happen in all the channels. At t = 5s, due to the boiling, pressure difference is created inside the MPHP. The pressure disturbance created in one channel will affect the other channel because of interconnection between all the channels.

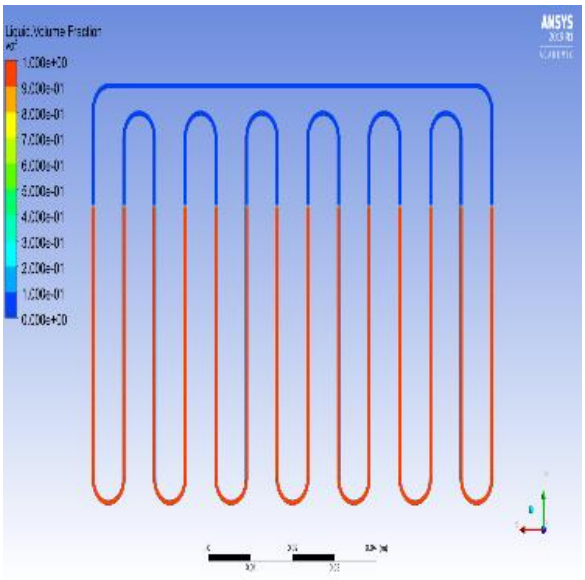

Figure 3: Liquid fraction contour for 0s.

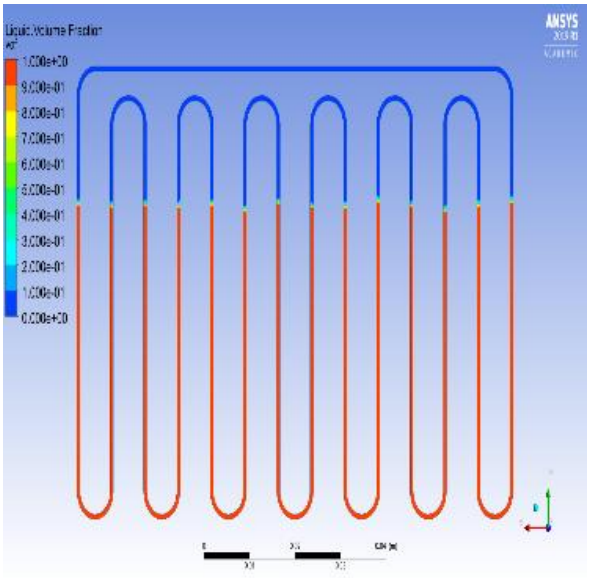

Figure 4: Liquid fraction contour for 1s.

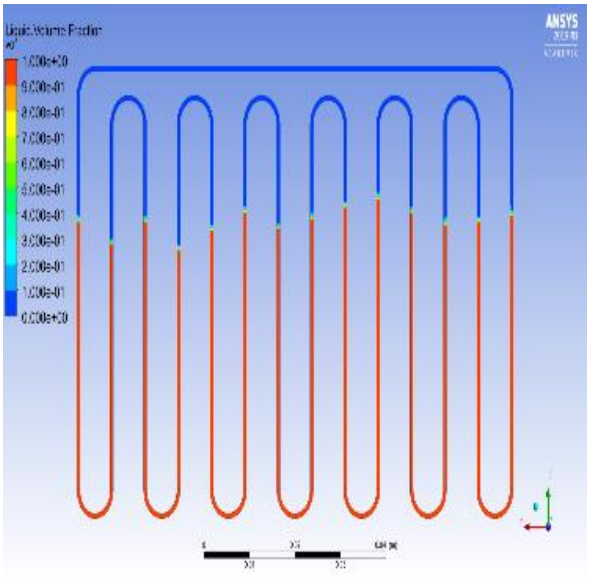

Figure 5: Liquid fraction contour for 5s.

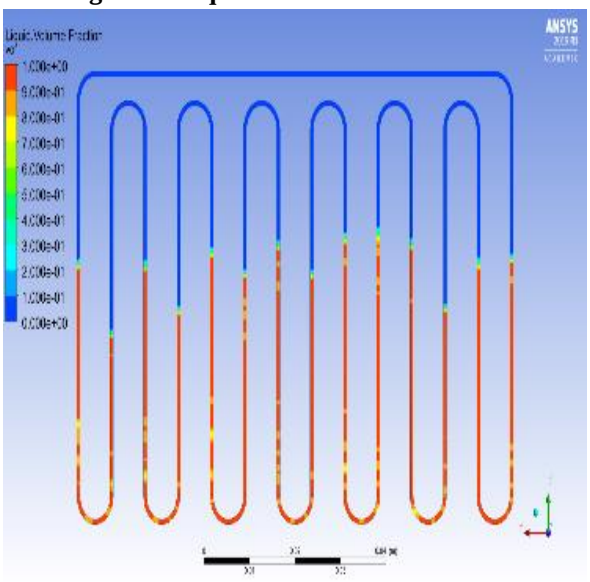

Figure 6: Liquid fraction contour for 8s.

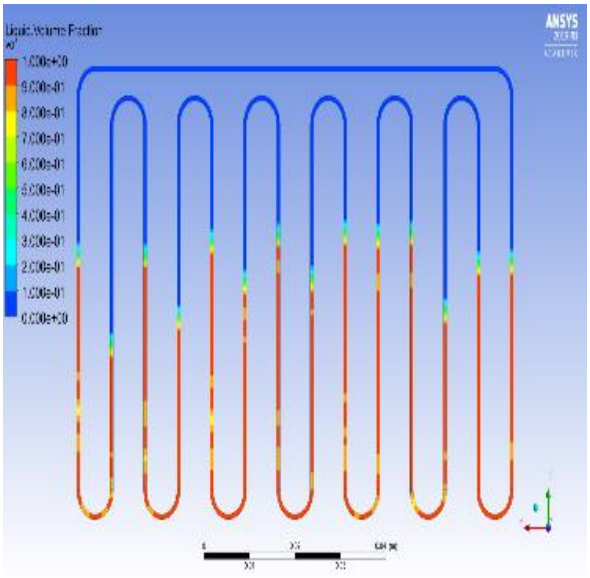

Figure 7: Liquid fraction contour for 10s.

Liquid fraction contour at t=8s, the vapor slug's formation is observed, which increases because of the boiling effect and the startup is observed. From the left side of computational domain, evaporator in the 4th U position and the corresponding channel shows the expansion liquid slugs because of vapor bubble created. At t = 10s, oscillation in MPHP is observed. Up to t = 22s, the sequence of oscillations and agglomeration of small vapor plugs to form a large one, are observed. At t = 26s number of vapor slugs got reduced since vapor plugs move towards the condenser section and get distorted. Since all the vapor plugs became sufficiently large and get collided by releasing the latent heat.

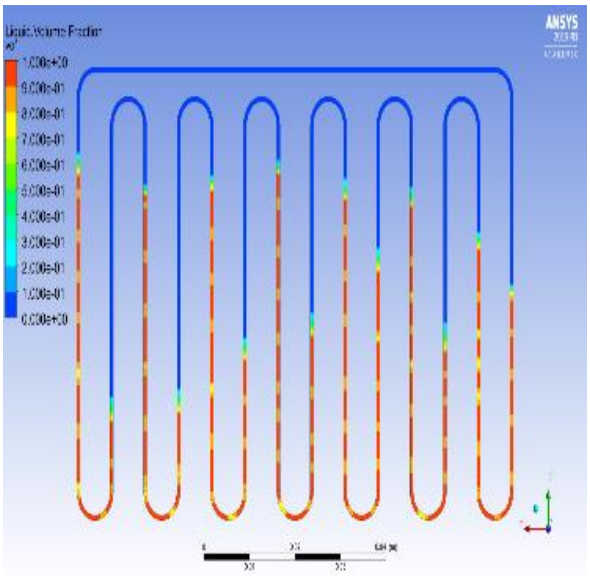

Figure 8: Liquid fraction contour for 22s.

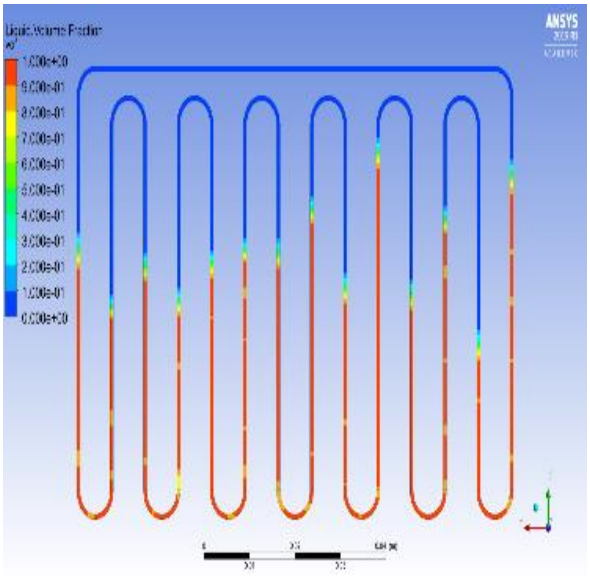

Figure 9: Liquid fraction contour for 26s.

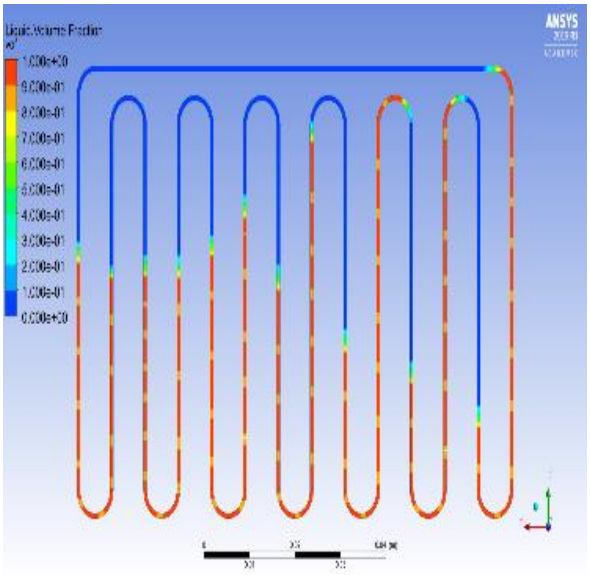

Figure 10: Liquid fraction contour for 45s.

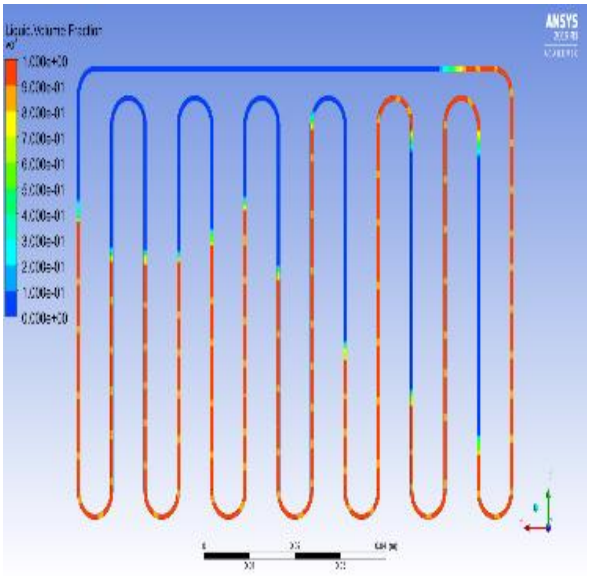

Figure 11: Liquid fraction contour for 60s.

Again, the cycle of forming small vapor plugs are started to form and it's observed in the contour. Oscillation amplitude i.e., displacement of liquid slugs and vapor plugs are different in different channel, this is because of different size of vapor plugs as well as the presence of different number of vapor plugs in individual channels of the computational domain. At t = 45s, agglomeration and collision of vapor plugs are occurred again and oscillation continues. The direction of fluid motion inside the MPHP is highly unpredictable, at t = 22s the flow tends to move in clockwise direction but at t = 45s flow changes to counter clockwise direction, this reversed again for t = 60s. Even if flow circulation is happening inside the MPHP, it will not follow the same direction; oscillation phase difference observed is high.

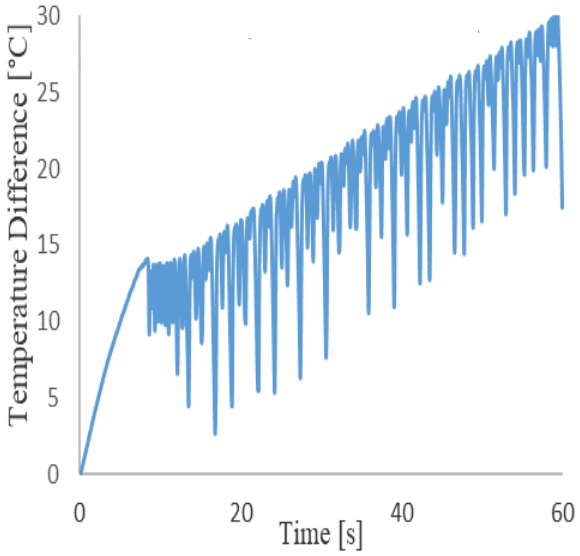

Figure 12: Temperature difference of MPHP

From the simulation result, it can be observed that flow inside the heat pipe is not continuous and tend to oscillate with respect to pressure disturbance created inside the loop as a result of input heat flux. This is the reason behind oscillating temperature profile. Figure 12 shows the variation of temperature profile of MPHP. Startup time observed is around 8 s to create required pressure difference inside the MPHP. Fluctuations in temperature are clearly observed and it indicates the flow oscillations prevailed in MPHP.

Table 1 Values of thermal resistance

S. No.	Heat input (W)	Thermal Resistance (K/W)
1	4.8	3.65
2	3.6	3.752
3	2.4	3.825
4	1.2	3.94

Table 1 brief about the values of thermal resistance attained by MPHP for four different heat inputs. From table 1, its observed that thermal resistance follows a conventional heat pipe pattern i.e., on increasing heat input thermal resistance will decrease.

IV. CONCLUSION

Following conclusions are the outcome of the computational investigation on MPHP,

- Startup time required for flow oscillations to occur is 8 seconds.
- Flow circulation inside the MPHP system is also observed along with flow oscillations.
- Flow circulation inside the MPHP system is not unidirectional and it tends to shift from clock wise to anti-clock wise and vice versa frequently.
- Oscillation amplitude is not same in all the channels, this is because of the pressure disturbance created inside each and every adjacent channel is different.
- On increasing heat input, MPHP thermal resistance start to decrease and this trend is similar to that of conventional PHP.

REFERENCES

1. S. M. Sohel Murshed and C. A. Nieto de Castro, "A critical review of traditional and emerging techniques and fluids for electronics cooling," *Renew. Sustain. Energy Rev.*, vol. 78, pp. 821–833, Oct. 2017.
2. H. Akachi, "United States patent," *Geothermics*, vol. 14, no. 4, pp. 595–599, 1985.
3. J. Qu, H. Wu, P. Cheng, Q. Wang, and Q. Sun, "Recent advances in MEMS-based micro heat pipes," *Int. J. Heat Mass Transf.*, vol. 110, pp. 294–313, 2017.
4. B. Suman, *Microgrooved Heat Pipe*, vol. 41, no. 08. Elsevier Masson SAS, 2009.
5. J. E, X. Zhao, Y. Deng, and H. Zhu, "Pressure distribution and flow characteristics of closed oscillating heat pipe during the starting process at different vacuum degrees," *Appl. Therm. Eng.*, vol. 93, pp. 166–173, Jan. 2016.
6. S. M. Pouryoussefi and Yuwen Zhang, "Nonlinear Analysis of Chaotic Flow in a Three-Dimensional Closed-Loop Pulsating Heat Pipe," *Appl. Therm. Eng.*, vol. 98, pp. 1–30, 2016.
7. S. M. Pouryoussefi and Y. Zhang, "Analysis of chaotic flow in a 2D multi-turn closed-loop pulsating heat pipe," *Appl. Therm. Eng.*, vol. 126, pp. 1069–1076, 2017.
8. *Intel® Xeon® Processor Scalable Family, Thermal Mechanical Specifications and Design Guide*. 2018.

AUTHORS PROFILE

A Bakhirathan received the bachelor's degree in Mechanical Engineering from Anna University, Tamil Nadu, India, in 2014, and master's degree in Heat Power Engineering in Anna University, Tamil Nadu, India, in 2017. He is currently a Research Scholar with Mechanical Engineering Department, NIT Calicut, Kerala, India.

Giridhar R received the bachelor's degree in Mechanical Engineering from Anna University, Tamil Nadu, India, in 2016. He pursued his master's degree in Energy Engineering and Management in NIT Calicut, Kerala, India.

K D P Pavan Kumar received the bachelor's degree in Mechanical Engineering from JNTU Kakinada, Andhra Pradesh, India, in 2017. He is pursuing his master's degree in Thermal Sciences in NIT Calicut, Kerala, India.

Gangadhara Kiran Kumar L received the master's degree and Ph.D. degree from IIT Guwahati, Assam, India. He is currently an Assistant Professor with Mechanical Engineering Department, NIT Calicut, Kerala, India, where he is also an In-charge and a Founding Member of the Computational Fluid Dynamics (CFD) laboratory. He also has profound knowledge and experience in the area of Fluid Flow and Heat Transfer and Computational Fluid Dynamics. His current research interest includes Micro/Nano Fluidics and Heat Transfer.